Thermal Aspects of Long-Term Propellant Storage on the Moon

TIBOR BUNA*
Martin Company, Baltimore Division, Baltimore, Md.

The passive thermal control aspects of above-surface storage of propellants on a lunar equatorial site are examined. A method is developed for predicting vaporization rates, mean temperatures, and temperature amplitudes of insulated propellants exposed to stabilized-periodic heating in the lunar environment. It is shown that, with the modest investment in required insulation weights, propellant temperature levels comparable to earth-ambient temperatures could be maintained indefinitely on the lunar surface, and boiloff rates of cryogenic propellants could be kept within acceptable limits for storage times up to several lunar cycles. The feasibility of artificially modifying the effective reflectivity of the lunar surface is demonstrated, and the effect of such modification on performance is evaluated. The relative effects of surface optical properties, insulation-heat-transfer mechanism (conduction vs radiation), and the spatial and temporal distribution of the environmental radiation intercepted by the container are discussed in the light of various insulation concepts.

Nomenclature

a = insulation constant, defined by Eq. (25)
dA = elemental area, ft²
A = tank surface area, ft²
ΔA = portion of tank surface exposed to radiation, ft²
b = insulation constant, defined by Eq. (25)
c = specific heat of propellant, Btu/lb-°R
c_i = specific heat of insulation, Btu/lb-°R
$D(r)$ = lunar radiation distribution function, defined by Eq. (9)
E = emissivity factor, defined by Eq. (32), dimensionless
E_0 = emissivity factor, ft; $= E\Delta x$
f = parameter defined by Eq. (28), dimensionless
F = view factor, dimensionless
h = height of center of tank above lunar surface, ft
k = point-thermal conductivity of insulation, Btu/ft-hr-°F
m = propellant mass per tank surface area, psf
n = number of layers in multilayered insulation
$\bar{N}$ = surface normal vector
P = period of lunar cycle, hr; = 708.73
$\dot{Q}$ = heat flux per unit area, Btu/ft²-hr
r = radius of circular area, ft, defined in Fig. 5
R = radius of spherical tank, ft
S = solar constant on lunar surface, Btu/ft²-hr-°R⁴; = 442.8
$\bar{S}$ = unit vector in direction of sun
t = time, hr
Δt = duration of heating period during cycle, hr (Fig. 6)
T = temperature, °R
ΔT = temperature amplitude, °R
x = distance from inner surface of insulation, ft
Δx = insulation thickness, ft, except as noted
α = solar absorptivity
ϵ = emissivity
β = angle between solar and vertical planes of surface normal (Fig. 2), except as noted
γ = angle between vertical (on lunar surface) and surface normal (Fig. 2)
ρ = density of propellant, lb/ft³
ρ_i = density of insulation, lb/ft³
ν = albedo of lunar surface; assumed 0.095
Φ = solar azimuth angle
σ = Stefan-Boltzmann constant, 0.1712×10^{-8} Btu/hr-ft²-°R
η = parameter defined by Eq. (29)
ξ = parameter defined by Eq. (27)
ψ = parameter defined by Eq. (13a)

Special symbols

$(\overline{\ })_A$ = averaged over tank area, A
$(\overline{\ })_P$ = averaged over period, P
$(\overline{\ })_{A,P}$ = averaged over both tank area and lunar period
$'$ and $''$ = conditions with uneven and even radiant heating, respectively (Fig. 6)

Subscripts

a = absorbed
A = albedo
dA = applied to elemental surface, dA
i = incident
L = lunar
m = mean
0 = at inner surface of insulation
S = solar
sat = saturation
sph = as applied to the spherical tank
tr = transferred through insulation
u = unit
Δx = at outer surface of insulation

Introduction

THE storage of propellants on the moon for extended periods of time eventually will become routine, with the advent of lunar-based space operations. The various aspects of the problem, as applied to storage times up to a limited number of lunar cycles, have been discussed in a previous work.[1] The purpose of this paper is to investigate the thermal aspects of above-surface storage of chemical propellants for periods that are large, as compared with the duration of the lunar cycle, so that the effects of initial transients can be neglected and the theory of stabilized periodic heat transfer applied. Attention is focused on heat-transfer rates, mean temperatures, and temperature amplitudes as functions of radiation geometry and insulation parameters. With the exception of the discussion of a specialized case, no effort will be directed toward determining instantaneous transfer rates or temperatures at any specified time.

It is noted that a thermal protection system designed to operate under the stabilized periodic condition does not necessarily meet performance requirements during all possible initial transients. The latter may vary considerably from case to case, depending on initial conditions, such as the temperature distribution in the insulation blanket at the time of landing. The significance of the stabilized periodic analy-

* Engineering Specialist, Propulsion and Thermodynamics Department. Member AIAA.

Presented as Preprint 2690-62 at the ARS 17th Annual Meeting and Space Flight Exposition, Los Angeles, Calif., November 13–18, 1962; revision received May 13, 1964.

sis is that it represents a limiting condition approached by all systems and that, from the point of view of evaluating thermal control techniques, it is more amenable to generalizations than the initial transient case.

Propellant Criteria

The permissible temperature levels and heating rates are established on the basis of chemical and physical stability, allowable vapor pressures with regard to container design, and engine criteria, such as engine pump inlet requirements or solid rocket burning-rate tolerances. The acceptable heating rates of volatile propellants are determined from tradeoffs between boiloff and insulation weight penalties.

Liquid propellants that can be stored in the earth environment without the use of any passive or active thermal control will be called "storables" (or "room-temperature") propellants, even though they require passive thermal insulation on the moon. Cryogenics require either insulation or refrigeration to be maintained in a liquid state.[2]

An examination of the fluctuation amplitudes of radiation intensities on the lunar surface (Fig. 1) provides convincing evidence that no presently known chemical propellants could be stored above-surface on an equatorial site without thermal protection; but the mean temperatures and temperature amplitudes which can be maintained by simple passive thermal control are comparable to earth-ambient temperature levels. However, an essential difference in the respective thermal interactions must be noted. In the all-radiation environment of the moon, the equilibrium temperature of a surface is a strong function of its orientation, and this may result in highly uneven temperature distributions on any three-dimensional object. On earth, the mechanism of heat transfer is primarily by convection and conduction, and the spatial temperature distribution is smoothed out by the presence of an atmosphere.

An uneven temperature distribution in a solid rocket may be especially harmful, since it may cause undesirable thermal stresses or uneven burning rates. Therefore allowable storage temperature limits and temperature gradients for solid rockets should be re-evaluated for lunar applications. In liquid propellants, temperature gradients coupled with density stratification[3, 4, 17] may occur with uniform or nonuniform heating or cooling. The tendency is for a cold layer to collect on the bottom of the tank and a warm layer to form at the liquid-vapor interface. Stratification reduces the effective thermal mass of the propellant that can absorb or give up heat by sensible heating or cooling within prescribed limits of vapor pressure. This subject requires further study as applied to lunar storage, but such studies are beyond the scope of this paper.

In view of the foregoing, the heat-transfer analysis is extended over two basic geometries: 1) the insulated sphere, representing liquid propellant storage containers, and 2) the insulated composite slab of arbitrary orientation, representing isolated sections of solid motors. In the latter case, it is assumed that the composite slab formed by an arbitrary small element of the motor casing and the liner, propellant, etc. attached to it, does not communicate thermally with the rest of the motor; it receives or gives up heat only through its insulated surface. The slab, as well as the sphere, is assumed to have infinite thermal conductivity, as compared to that of the insulation blanket. Heat transfer through the latter is assumed to be one-dimensional.

Lunar Surface and Environment Characteristics

Our present state of knowledge with regard to lunar environment and surface characteristics has been reviewed in detail in the literature.[5] The purpose here is briefly to summarize those factors pertinent to the basic assumptions in the analysis.

The upper limit of the density of the moon's atmosphere has been reported as 10^{-13} times earth's atmospheric density. This is several orders of magnitude lower than the vacuum requirements of high-performance, multilayered insulations,[6, 7] which may therefore be used without apparent difficulty for lunar applications. Thus the thermal environment of the moon is an all-radiation environment, which may be graphically represented by giving the equilibrium temperatures of exposed surfaces of known optical properties as functions of time and orientation. Such curves are shown in Fig. 1, for α/ϵ ratios of 3.0 and 0.264; the first represents weathered aluminum, and the second is indicative of the state of the art with regard to practically attainable solar reflectors.[8] [The curves were calculated on the basis of Eqs. (20–24), to be discussed later.] These curves indicate that an uninsulated object may experience temperature variations in time and across its surface area which are of the same order of magnitude as its average temperature. The temperature of the surface facing downward is very little affected by changes in surface optical properties, since it receives mostly infrared radiation from the lunar surface, whereas the surface facing upward receives only solar radiation.

The maximum and minimum temperatures of the lunar surface, as measured by Pettit and Nicholson[9] and Pettit,[10] are 668°R at the subsolar point and 216°R near the east limb, in the shadow. The distribution of planetary heat across the disk of the full moon does not follow Lambert's cosine law but rather the $\frac{2}{3}$ power of the cosine of the phase angle.[9] However, to avoid unnecessary complications in the analysis, Lambert's law is assumed herein to apply to a small

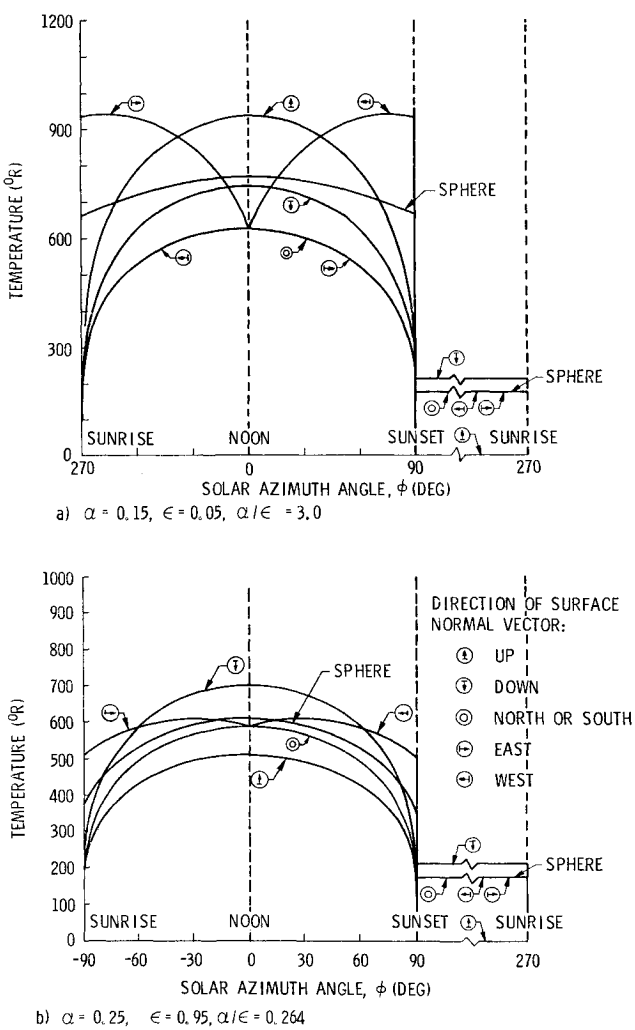

Fig. 1 Equilibrium surface temperatures.

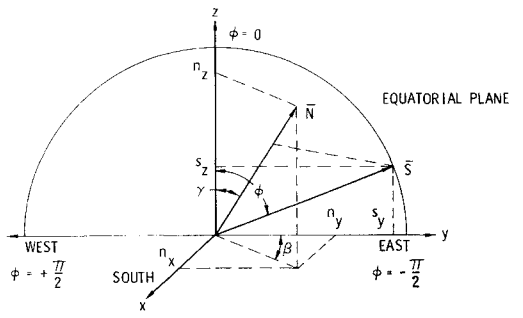

Fig. 2 Definition of geometrical orientation parameters.

area. The apparent fast temperature response of the lunar surface, as evidenced by both the rapid temperature variations during eclipses[10] and the fact that the maximum temperature occurs at the subsolar point without a phase lag, has led to the assumption in the present analysis that the lunar surface is in radiation equilibrium with the incident solar flux. The albedo of the moon is very low; a representative value of 0.095 has been assumed. Since we have no current knowledge concerning lunar surface roughness in terms of dimensions comparable to the dimensions of the propellant tanks, the surface is assumed to be flat.

Radiation Geometry

This section is devoted to the development of solar and lunar view factors for the two basic geometries considered, namely, the sphere and the slab of arbitrary orientation. It is assumed that the sun is a point source of radiation at infinite distance, that the lunar surface is an infinite flat plane, and that Lambert's law applies. The solar and lunar view factors of an element dA of the container surface are defined as the fractions of radiation emitted by dA that are incident on the sun and the lunar surface, respectively. With the geometrical orientation parameters, as defined on Figs. 2 and 3, when $F_{dA} > 0$,

$$F_{dA,\,S} = \bar{S}\cdot\bar{N} = s_x n_x + s_y n_y + s_z n_z = \cos\gamma\cos\Phi - \sin\gamma\cos\beta\sin\Phi \quad (1)$$

$$F_{dA,S} = \cos\theta \qquad \text{(Lambert's Law)} \quad (2)$$

$$F_{dA,L} = (1 - \cos\gamma)/2 \quad (3)$$

The view factors of the sphere may be obtained by integration of Eqs. (2) and (3) [see Ref. 11 regarding Eq. (3)]. With the notations of Fig. 3,

$$F_{\text{sph},S} = \frac{1}{A}\int_0^{\pi/2} F_{dA,S}\,dA = \frac{1}{2}\int_0^{\pi/2}\sin\theta\cos\theta d\theta = \frac{1}{4} \quad (4)$$

which is valid for $-(\pi/2) \leq \Phi \leq (\pi/2)$, and

$$F_{\text{sph},L} = \frac{1}{A}\int_0^{\pi} F_{dA,L}\,dA = \frac{1}{4}\int_0^{\pi}(\sin\gamma - \cos\gamma\cdot\sin\gamma)d\gamma = \frac{1}{2} \quad (5)$$

valid for $-(\pi/2) \leq \Phi \leq (3\pi/2)$. Thus a sphere receives one-quarter as much radiation from the sun as a flat plate of equal area with its normal pointing toward the sun, and it receives one-half as much radiation from the lunar surface as does a flat plate of equal area facing the lunar surface.

It is of some practical interest to ask how much of the total lunar radiation incident on the sphere originates from within a circular area of arbitrary radius r and center coincident with the projection of the center of the sphere on the lunar surface. For the answer, the view factor of the circular area of radius r, with respect to the sphere of radius R, is first developed. For this purpose, Nusselt's double projection principle[11] is applied to obtain the view factor between the sphere and a small elemental surface dA, as shown in Fig. 4:

$$F_{dA,\,\text{sph}} = \overline{BC}\cdot(\overline{B'C'})/R_u^2 = (R/h)^2\cos^3\theta \quad (6)$$

Noting, from Fig. 4, that

$$dA = rd\beta dr \qquad r = h\tan\theta \qquad dr = h\sec^2\theta d\theta \quad (7)$$

$$F_{\pi r^2,\text{sph}} = \frac{1}{\pi r^2}\int_0^{\theta}\int_0^{2\pi}(R/h)^2\cos^3\theta h^2\tan\theta\sec^2\theta d\beta d\theta = 2(R/r)^2(1-\cos\theta) \quad (8)$$

Thus,

$$D(r) \equiv \frac{\text{radiation from } \pi r^2}{\text{radiation from lunar surface}} = 1 - \cos\theta = 1 - (1 + r^2h^{-2})^{-1} \quad (9)$$

The lunar radiation distribution function, Eq. (9), is plotted with r/h as abscissa in Fig. 5. The surprising result of this analysis is that approximately 90% of the lunar radiation incident on a spherical tank originates from within an area of radius of only about 10 times the height of the center of the tank above the lunar surface.

It follows that change in the lunar surface characteristics in the vicinity of the storage tank may significantly affect the nature of incident lunar radiation on the tank. Such changes may be caused, for example, by the exhaust plumes of a landing rocket, or they may be effected deliberately in order to increase the reflectivity of the lunar surface.

An increase in the moon's albedo is desirable, since the absorption of the reflected solar radiation can be controlled by proper selection of the optical properties of the tank surface, whereas the absorption of lunar-emitted radiation in its original infrared wavelength is rather insensitive to the optical properties of the receiver. The effective albedo of the lunar surface may be increased by using a relatively moderate-size reflective "carpet" under the storage tank (see also Dempster et al.[16]). Finally, by use of Fig. 5, the relative effects of the tank's shadow on the incident radiation at the subsolar points may be evaluated. For example, for the case where $h = R$, the tank's shadow at noon cuts out approximately 30% of the lunar radiation, whereas for the case $h = 2R$, the reduction is only about 10%.

Heat Transfer Analysis

General Theory

Consider an insulated propellant container of thickness Δx and let T_0 and $T_{\Delta x}$ be the inner- and outermost surface temperatures, respectively, of the insulation blanket. T_0 and $T_{\Delta x}$ are generally functions of both time and space but may be assumed to be uniform, at any given time, over a small

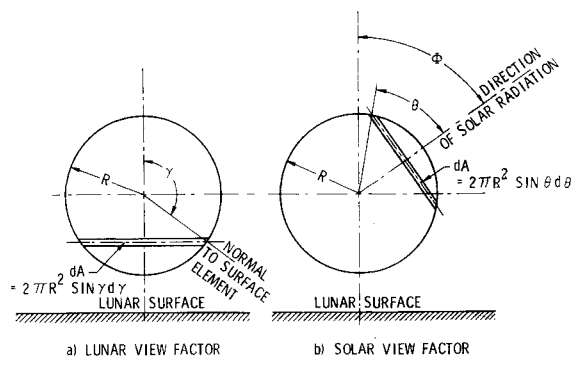

Fig. 3 Determination of integrated view factors of sphere.

elemental area dA. Further, let Δx be small, compared to the dimensions of the container, and consider the circumferential heat flow within the insulation to be negligible, so that one-dimensional heat transfer applies. Thus

$$\frac{\partial}{\partial x}\left(k\frac{\partial T}{\partial x}\right) = -\rho_i c_i \frac{\partial T}{\partial t} \tag{10}$$

where $k = k(T)$ and $T = T(x, t)$. We note that the point-thermal conductivity k of the insulation may be an arbitrary function of temperature—but of temperature only. The latter requirement is satisfied by most insulation concepts of interest (exceptions are insulations that are transparent or partially transparent to radiation, e.g., a thin layer of perlite[12]; for these, k is also a function of x). The boundary conditions for Eq. (10) are

$$T = T_0 = \text{const} \qquad (x = 0, \text{ state changes}) \tag{11a}$$

$$\left(k\frac{\partial T}{\partial x}\right)_0 = mc\frac{dT}{dt} \qquad (x = 0, \text{ sensible heat changes}) \tag{11b}$$

$$\left(k\frac{\partial T}{\partial x}\right)_{\Delta x} = \dot{Q}_a - \epsilon\sigma T_{\Delta x}^4 = \dot{Q}_{tr} \qquad (x = \Delta x) \tag{11c}$$

In Eq. (11b), it was assumed that the heat is distributed uniformly within a mass m of the propellant and that this mass is the only portion of the propellant responding to the heat flow through the insulation blanket of area dA.

For the stabilized periodic condition, the time-integral of Eq. (10) over a full period yields

$$\int_t^{t+P}\frac{\partial}{\partial x}\left(k\frac{\partial T}{\partial x}\right)dt = \int_t^{t+P}\rho_i c_i\frac{dT}{dt}\,dt = 0 \tag{12}$$

since, over a full period, the accumulation of heat within an elemental thickness dx of the insulation vanishes.

We now introduce a new parameter, $\psi = \psi(T)$, and its averages over time and/or area, as follows:

$$\psi \equiv \int_0^T k\,dT \quad \text{or} \quad k = \frac{d\psi}{dT} \quad \text{and} \quad \left(k\frac{\partial T}{\partial x}\right) = \frac{dQ}{dt} = \frac{\partial \psi}{\partial x} \tag{13a}$$

$$(\bar{\psi})_P \equiv \frac{1}{P}\int_t^{t+P}\psi dt = \frac{1}{P}\int_t^{t+P}\int_0^T k\,dT\,dt \tag{13b}$$

$$(\bar{\psi})_{P,A} \equiv \frac{1}{A}\int_0^A (\bar{\psi})_P dA = \frac{1}{PA}\int_0^A\int_t^{t+P}\int_0^T k\,dT\,dt\,dA \tag{13c}$$

Substituting Eq. (13a) into Eq. (12), applying Leibnitz's rule[13]

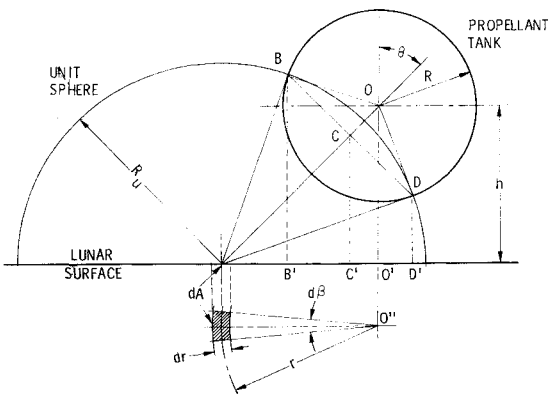

Fig. 4 Radiation geometry for derivation of D (r).

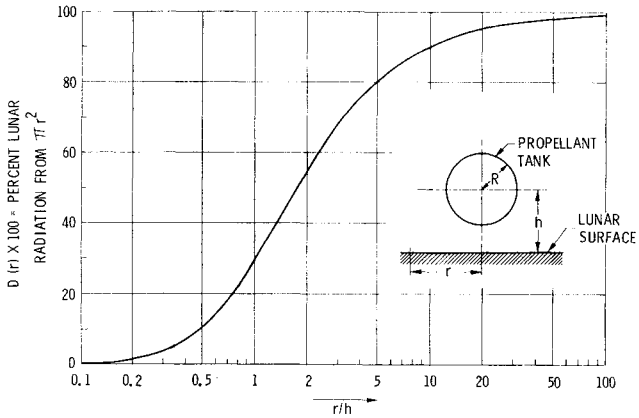

Fig. 5 Lunar radiation distribution function.

twice, and using the definition of $(\bar{\psi})_P$ from Eq. (13b), the differential equation reduces to

$$\partial^2(\bar{\psi})_P/\partial x^2 = 0 \tag{14}$$

and its solution is

$$\frac{\partial(\bar{\psi})_P}{\partial x} = \text{const} = (\bar{Q}_{tr})_P = \frac{(\bar{\psi}_{\Delta x})_P - (\bar{\psi}_0)_P}{\Delta x} \tag{15}$$

Equation (15) gives the average heat-transfer rate within a lunar cycle, for a small surface element dA of the insulation. For the entire area A,

$$(\bar{Q}_{tr})_{P,A} \equiv \frac{1}{A}\int_A (\bar{Q}_{tr})_P dA = \frac{(\bar{\psi}_{\Delta x})_{P,A} - (\bar{\psi}_0)_{P,A}}{\Delta x} \tag{16}$$

Hence, the significance of the parameter ψ is that its averages over time and surface area determine the average heat transfer rates per period of lunar cycle. For a cryogenic stored in a vented tank at constant pressure, $T_0 = T_{sat} = \text{const}$, and

$$(\bar{\psi}_0)_{P,A} = \int_0^{T_{sat}} k\,dT \tag{17}$$

For a room-temperature propellant, in the absence of heat production or sink inside the tank, the net heat transfer to the propellant during a full period is zero; hence, from Eqs. (16) and (13a):

$$(\bar{\psi}_0)_{P,A} \equiv \int_0^{T_m} k\,dT = (\bar{\psi}_{\Delta x})_{P,A} \tag{18}$$

where T_m is the "mean" temperature of the propellant and may be obtained as the inverse transform of $(\bar{\psi}_{\Delta x})_{P,A}$, which in turn is determined by the point thermal conductivity of the insulation and the outer skin temperature profiles. It will be shown later that T_m may differ considerably from the arithmetic average of the outer skin temperature.

A determination of $(\bar{\psi}_0)_{P,A}$ will establish not only the mean temperature but also the amplitude ΔT of the temperature fluctuations of the room-temperature propellants. The amplitude may be estimated from the following considerations. It is evident (Fig. 1) that the outer-surface temperature levels during the lunar night are vanishingly small as compared with the levels during the day, and that the heating and cooling periods during a full lunar cycle are approximately equal. Thus for well-insulated tanks, when $\Delta T \ll T_m$,

$$2\Delta T = (\bar{\psi}_0)_{P,A}P/2mc\Delta x \tag{19}$$

Consequently, the maximum and minimum temperatures are approximately $T_m + \Delta T$, and $T_m - \Delta T$, respectively. In Eq. (19) it was assumed that, during the cooling period (lunar night), the outer-surface temperature of the insulation is essentially zero.

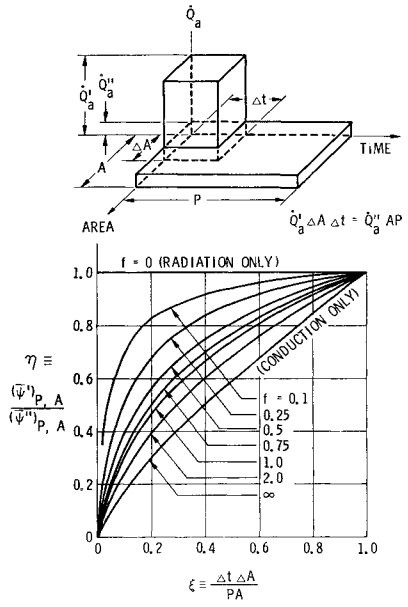

Fig. 6 Effect of radiation distribution on heat transfer.

For a complete definition of the heat-transfer problem, $(\bar{\psi}_{\Delta x})_{P,A}$ remains yet to be determined; it may be calculated from the outer skin temperature profiles which, in turn, may be determined from heat balance considerations. This heat balance on the outer surface of the insulation may be considerably simplified by taking advantage of the fact that for well-insulated propellant containers, $\dot{Q}_{tr} \ll \dot{Q}_a$. Hence, for a surface element dA, from Eq. (11c),

$$T_{\Delta x} \cong (\dot{Q}_a/\epsilon\sigma)^{1/4} \tag{20}$$

The implicit assumption that the outermost surface of the insulation is in radiation equilibrium with the environment is conservative, since the small error introduced by neglecting $\dot{Q}_{tr}$ in Eq. (11c) tends to increase the temperature difference across the insulation blanket. $\dot{Q}_a$ may be determined from radiation geometry and lunar heat balance considerations as follows.

The assumed zero thermal conductivity of the lunar surface implies that, of the (S cosΦ) Btu/ft^2-hr incident solar flux on the lunar surface, νS cosΦ is reflected as albedo in the solar wavelength and $(1 - \nu)S$ cosΦ is absorbed and immediately re-radiated in the infrared wavelength. With the help of this lunar heat balance and Eqs. (1–3), the heat absorbed by a surface element dA, of unit area, may be expressed as follows:

For $-\pi/2 \leq \Phi \leq \pi/2$ (lunar day),

$$\dot{Q}_{a,dA} = S\{\alpha F_{s,dA} + [\alpha\nu + (1 - \nu)\epsilon]F_{L,dA}\cos\Phi\} \tag{21}$$

and for $\pi/2 \leq \Phi \leq 3\pi/2$ (lunar night),

$$\dot{Q}_{a,dA} = \epsilon\epsilon_L\sigma T_L{}^4 F_{dA,L} \tag{22}$$

Similarly, the average heat absorption per unit area of a sphere may be computed as follows:

For $-\pi/2 \leq \Phi \leq \pi/2$ (lunar day),

$$(\bar{\dot{Q}}_a)_{sph} = S\left\{\tfrac{1}{2}[\nu\alpha + \epsilon(1 - \nu)]\cos\Phi + \frac{\alpha}{4}\right\} \tag{23}$$

and for $\pi/2 \leq \Phi \leq 3\pi/2$ (lunar night),

$$(\bar{\dot{Q}}_a)_{sph} = \epsilon\epsilon_L\sigma T_L{}^4/2 \tag{24}$$

The use of Eqs. (23) and (24) in conjunction with Eq. (20) will give an average outer surface temperature that is representative of a spherical shell of infinite thermal conductivity. This may be considered as the limiting case for an insulated container enclosed in a heavy meteoroid shield. In the other extreme, the outer layer of a multilayered insulation blanket may have negligible circumferential conductance. In this case $\psi_{\Delta x}$, as determined by the use of Eqs. (20–22) and (13a), must be integrated over the entire surface area of the tank system.

Effect of Distribution of Absorbed Radiation

Let the outermost surface of an insulation blanket of area A be subjected to periodic radiant heating as in the following two cases (see Fig. 6):

Case I.

During a full period P, the radiation is impinging only on a surface element $\Delta A < A$ for a time $\Delta t < P$, during which the surface element is maintained at a temperature T' by absorbing (and re-radiating) a heat flux $\dot{Q}_a'$, so that the total radiation absorbed (and re-radiated) by the surface element during the whole cycle is $\dot{Q}_a' \Delta A \Delta t$.

Case II.

The same total radiation absorbed by the surface is evenly distributed over the whole surface area A and through the full period P.

We shall compare the heat transfer aspects of the two cases by evaluating the respective $(\bar{\psi}_{\Delta x})_{A,P}$ or the ratio $(\bar{\psi}_{\Delta x}')_{A,P}/(\bar{\psi}_{\Delta x}'')_{A,P}$. Without loss of generality we may assume that the heat transfer through the insulation may be expressed as the sum of conduction and radiation, such that

$$\psi = aT + bT^4 \qquad \text{or} \qquad k = a + 4bT^3 \tag{25}$$

where a and b may assume arbitrary values. By definition

$$\psi_{\Delta x}' = aT' + b(T')^4 \qquad \text{and} \qquad \psi_{\Delta x}'' = aT'' + b(T'')^4 \tag{26}$$

We introduce the following notations:

$$\xi \equiv \Delta A(\Delta t)/AP \tag{27}$$

$$f \equiv aT'/b(T')^4 \tag{28}$$

$$\eta \equiv (\bar{\psi}_{\Delta x}')_{A,P}/(\bar{\psi}_{\Delta x}'')_{A,P} = \psi_{\Delta x}'(\Delta A)(\Delta t)/\psi_{\Delta x}''AP \tag{29}$$

Note that the insulation parameter f represents the ratio of conduction to radiation at the specified temperature T'. From Eqs. (20) and (27) it follows that

$$(T')^4 = (T'')^4/\xi \qquad \text{or} \qquad T' = T''/\xi^{1/4} \tag{30}$$

By substitutions from Eqs. (27, 30, and 28) into (29), we obtain

$$\eta = \xi\,\frac{b(T')^4(1 + f)}{b(T')^4[\xi + f\xi^{1/4}]} = \frac{1 + f}{1 + f\xi^{-3/4}} \tag{31}$$

Equation (31) is shown graphically on Fig. 6 and indicates that, for a given total incident and absorbed radiation heat flux during a full period, the parameter $(\bar{\psi}_{\Delta x})_{A,P}$ is larger for even than for uneven distribution of absorbed radiation in time and space. This effect increases with the ratio of conduction to radiation within the insulation; it is zero for the special case of an "ideal radiation shield," where $f = 0$. It may be noted from Eq. (27) that, with regard to their effects on $(\bar{\psi}_{\Delta x})_{A,P}$, the spatial and temporal distributions of the absorbed radiant flux are interchangeable.

The foregoing analysis indicates that the use of a heavy (high circumferential conductance) meteoroid shield will increase boiloff rates or mean temperatures and temperature amplitudes of the propellants. It also shows that the simplifying assumption of infinite circumferential conduction in the outermost layer of the insulation gives conservative results in the analysis. This assumption will be adopted

in the subsequent discussion of the commercial multilayered insulation system.

Properties of the Ideal Radiation Shield

For the ideal or "floating" radiation shield,

$$Q/A = \sigma E(T_h^4 - T_c^4) \tag{32}$$

where T_h and T_c are the hot- and cold-side temperatures, respectively, and the emissivity factor E is a function of the number and optical properties of the shields but is independent of temperature.[14] For a sufficiently large number of shields (say, $n > 25$), E may be written as $E = E_0/\Delta x$ where E_0 is a constant, and Δx is the number of shields multiplied by their spacing. Thus $\psi = \sigma E_0 T^4$, or

$$(\bar{\psi}_{\Delta x})_{P,A} = \frac{E_0\sigma}{A \cdot P}\int_P\int_A T_{\Delta x}^4 dA \cdot dt$$

$$(\bar{\psi}_0)_{P,A} = E_0\sigma T_0^4 \tag{33}$$

On the other hand, a heat balance on the outer surface of the insulation gives

$$(\bar{Q}_{tr})_{P,A} = (\bar{Q}_a)_{P,A} - \frac{1}{A \cdot P}\int_P\int_A \epsilon\sigma T_{\Delta x}^4 dA \cdot dt \tag{34}$$

and, by definition

$$(\bar{Q}_a)_{P,A} = \alpha[(\bar{Q}_{i,S})_{P,A} + (\bar{Q}_{i,A})_{P,A}] + \epsilon(\bar{Q}_{i,L})_{P,A} \tag{35}$$

Combining Eqs. (33–35) and (16) gives

$$(\bar{Q}_{tr})_{P,A} = \frac{E\epsilon}{E+\epsilon}\left\{\frac{\alpha}{\epsilon}[(\bar{Q}_{i,s})_{P,A} + (\bar{Q}_{i,A})_{P,A}] + (\bar{Q}_{i,L})_{P,} - {}_A\sigma T_0^4\right\} \tag{36}$$

The first term on the right-hand side of Eq. (36) may be expressed as

$$E\epsilon/(E+\epsilon) \equiv (1/E + 1/\epsilon)^{-1} \tag{37}$$

Furthermore, for

$$E \ll \epsilon \qquad \epsilon E/(E+\epsilon) \approx E = E_0/\Delta x \tag{38}$$

Thus the heat transferred per lunar cycle through an ideal radiation shield is inversely proportional to the insulation thickness and to an "over-all resistance" composed of the sum of the reciprocals of the emissivity factor and surface emissivity, and it is directly proportional to the incident flux on the outer surface and the α/ϵ ratio of the outer surface. It is independent of the distribution of the incident radiant flux on the outer surface with respect to time and surface-coordinates. This was predicted for the ideal radiation shield ($f = 0$) in the preceding section, and it is also evident from the fact that Eqs. (33) and (34) both contain the surface temperature at the fourth power only. A term involving other than the fourth power of the temperature in the definition of ψ would result in the distribution effect discussed in the preceding section.

Application to Commercial Multilayered Insulation

Equations (16–24) are the principal working equations of the method. The present section presents the results of typical calculations based on these equations and as applied to the insulated slab of arbitrary orientation and the insulated sphere with infinite circumferential conduction in the outermost layer of the insulation.

The insulation used in the analysis was a typical Linde multilayered insulation, with point thermal conductivity given[15] as

$$k = 2.4 \times 10^{-7}T^{1/2} + 2.36 \times 10^{-13}T^3 \tag{39}$$

Thus

$$\psi = \int_0^T k dT = 1.6 \times 10^{-7}T^{3/2} + 0.59 \times 10^{-13}T^4 \tag{40}$$

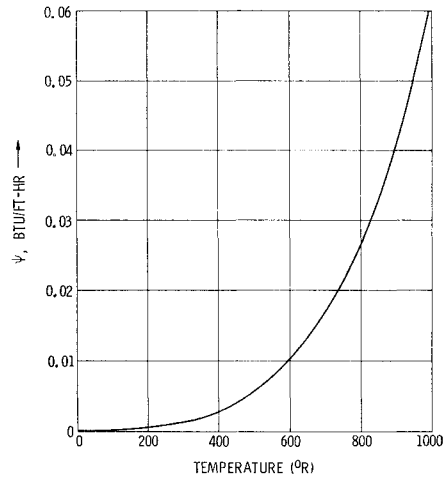

Fig. 7 ψ vs T for one multilayered insulation.

Equation (40) is plotted in Fig. 7. The values of $(\bar{\psi}_{\Delta x})_{A,P}$ for the various configurations discussed in this analysis were evaluated with the use of Fig. 7 and the equilibrium temperature profiles in Fig. 1. The calculation method is a straight averaging procedure. A typical example, using a finite-step integration procedure, is shown in Table 1 for the "slab pointing west." Also shown in the table are the computations of the propellant mean temperature and temperature amplitude for mc = 1 Btu/ft² − °R and Δx = 1 in. This example has also been used to test the accuracy of Eq. (19). Accordingly, the temperature profile of the propellant for one full cycle was calculated by the use of a small-perturbation technique.[1] The result is plotted in Fig. 8. It is noted that there is good agreement between the temperature amplitudes as predicted by Eq. (19) (and Table 1) and as determined from the temperature profile.

Figure 9, for the geometries indicated, shows the attainable propellant mean temperatures on the moon, as functions

Table 1 Calculation of $(\bar{\psi}_{\Delta x})_{P,A}$ for insulated slab pointing West; α/ϵ = 3.0, Linde insulation[15]

Φ	$T_{\Delta x}$ (from Fig. 1)		ψ (from Fig. 7)
−85	340		0.0017
−75	450		0.0039
−65	507		0.0057
−55	550		0.0075
−45	575		0.0087
−35	598		0.0099
−25	613		0.0107
−15	620		0.0125
−5	625		0.0132
5	680		0.0163
15	770		0.0237
25	825		0.0305
35	870		0.0375
45	900		0.0425
55	923		0.0463
65	937		0.0495
75	945		0.0510
85	940		0.0500
		Sub total	0.4211
90–270	175		0.0005

$$(\bar{\psi}_{\Delta x})P = \frac{\frac{0.4211}{18} + 0.0005}{2} = 0.01195 \text{ Btu/hr-ft}$$

T_m = 630°R (from Fig. 7)

For Δx = 1 in. and mc = 1 Btu/ft²-°R,

$$\Delta T = (\bar{\psi}_{\Delta x})P/4\,mc = 25.4°\text{R}$$

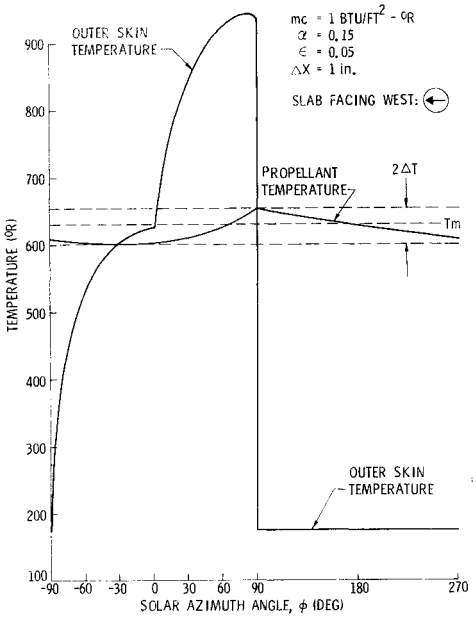

Fig. 8 Typical temperature profile of insulated slab.

of the α/ϵ ratio and lunar surface reflectivity (albedo). The mean temperatures obtainable with the various slab orientations tend to converge at $\alpha/\epsilon = 1$, except for the slabs pointing North or South. Note that the attainable temperature range may be considerably widened by the use of artificial albedos.

It should be pointed out here that the mean temperature depends only on $(\bar{\psi}_{\Delta x})_{A,P}$, whereas the insulation thickness controls the amplitudes of the temperature fluctuations. Figure 10 shows heat transfer rates to a spherical tank with one inch of insulation. The sloping lines give the heat-transfer rates to a hypothetical propellant at absolute zero temperature. These may be used with good approximation to calculate liquid hydrogen boiloff rates. Thus, at $\alpha/\epsilon = 3$ and albedo of 0.095, the heat-transfer rate to liquid hydrogen is 87.5 Btu/ft²-cycle. The heat-transfer rate to a room-temperature propellant at 520°R, all other conditions being the same, will be 87.5 − 52.5 or 35 Btu/ft²-cycle.

Figure 10 also indicates that, at low α/ϵ ratios, the performance of the thermal protection system may be considerably improved by the use of an artificial albedo. Representative numerical results, as obtained by the use of Figs. 9 and 10, Eq. (19), plus propellant data from Ref. 1, are shown in Table 2.

Finally, Fig. 11 verifies the statement made at the beginning of this paper, that the attainable temperature levels with insulated objects on the moon are comparable to earth-environmental temperatures. Furthermore, it indicates that the use of passive thermal control in cryogenic storage

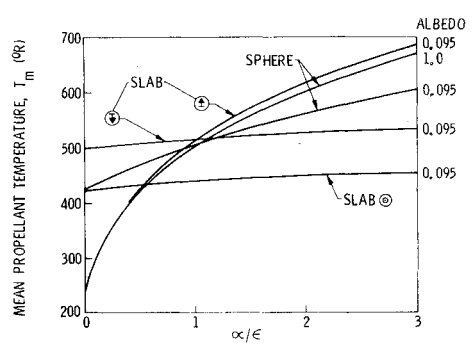

Fig. 9 Obtainable mean temperatures of insulated non-volatile propellants.

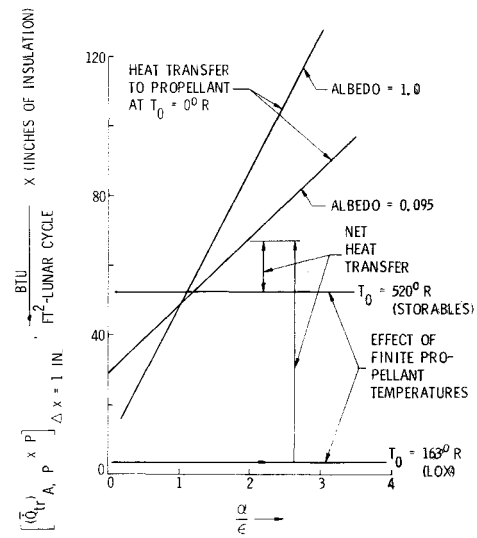

Fig. 10 Heat transfer to insulated sphere.

on the lunar surface is necessarily associated with vaporization loss. The latter may be kept within acceptable limits by using adequate thicknesses of insulation, which may be determined from Fig. 10, permissible boiloff rate, the tank size, and the latent heat of the propellant.

Conclusions

Extended storage of propellants on the lunar surface is thermally feasible by the use of one to several inches of commercial multilayered insulations and presently attainable surface optical properties. Earth-storable propellants may be maintained indefinitely in insulated containers, and boiloff rates of cryogenic propellants may be kept within acceptable limits for storage times up to several lunar cycles.

For well-insulated storable propellants ($\dot{Q}_{tr} \ll \dot{Q}_a$) under stabilized temperature cycling, the mean temperatures are functions of the surface optical properties of both the container and the lunar surface, as well as of the mechanism of heat transfer (conduction/radiation ratio) through the insulation blanket, but are independent of insulation thickness. The temperature amplitudes are inversely proportional to the insulation thickness. The heat-transfer rates to insu-

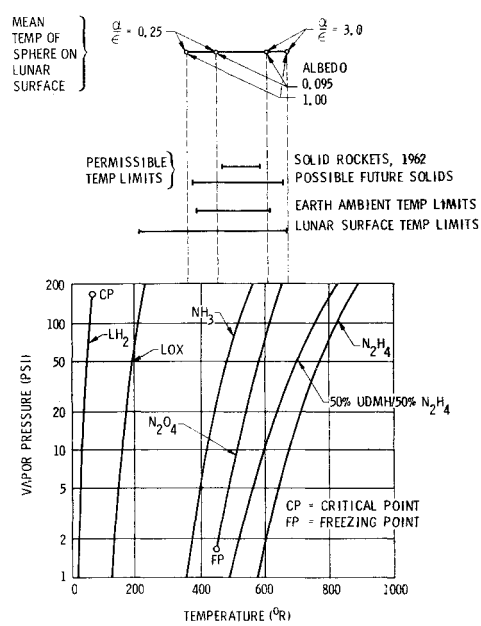

Fig. 11 Representative temperature levels.

Table 2 Representative results; spherical tank, 1-ft radius, 1-in. insulation[a]

	LH_2	LOX	N_2O_4	50/50 UDMH/N_2H_4	α/ϵ
Percent boiloff/cycle, evaporative heating	30.2	3.9	0.71	0.50	3.0
	16.8	2.1	0.0	0.0	1.0
Temperature rise, °R/cycle, sensible heating	26.5	8.7	3.4	3.1	3.0
	14.7	0.5	0.0	0.0	1.0
Temperature amplitude, °R, stabilized periodic sensible heating; $T_m = 505$°R	...	...	1.1	1.0	1.0

[a] For radius R and insulation thickness Δx, divide results by $R \cdot \Delta x$.

lated cryogenic propellants are proportional to the α/ϵ ratio of the outermost surface of the insulation and inversely proportional to the insulation thickness.

The heat-transfer rate per cycle through an ideal, or "floating," radiation shield is proportional to the total radiation flux intercepted by the outermost surface but is independent of the distribution of this flux in time and over the surface area. The performance of "real" insulations, on the other hand, depends quite strongly on the spatial and temporal distribution of intercepted radiation. In general, even distribution maximizes heat-transfer rates, mean temperatures, and temperature amplitudes. Thus, the addition of a heavy meteoroid shield to an insulation system will have the tendency to increase the boiloff rates of cryogenic propellants and the mean temperatures and temperature amplitudes of room-temperature propellants.

Changes in the radiation properties of the lunar surface in the vicinity of the tank may affect the heat-transfer characteristics significantly, which points to the possibility of using reflective "carpets" to increase artificially the effective albedo of the lunar surface.

An approximate method has been developed for calculating the mean temperatures, temperature amplitudes, and boiloff rates of insulated propellants under stabilized periodic heating on the lunar surface. Equations (16–24) are the working equations of the procedure. The distribution of heat and temperature inside a propellant container requires further study with respect to stratification in liquid propellant tanks and thermal stresses and temperature gradients in solid rockets.

References

[1] "Earth lunar transportation system—lunar propellant storage," Martin Co. ER 12387-I, Contract NAS 8-1531, Task no. 2, NASA George C. Marshall Space Flight Center (May 1962).

[2] Grelecki, G. J. and Tannenbaum, S., "Survey of current storable propellants," ARS J. **32**, 1189–1195 (1962).

[3] Webster, T. J. and Robb, J., "Factors Affecting the design of high-pressure liquefied gas storage tanks," *Proceedings of 1961 Cryogenic Engineering Conference* (Plenum Press, Inc., New York, 1962), pp. 143–148.

[4] Bailey, T., Van De Koppel, R., and Skartvedt, G., "Cryogenic propellant stratification analysis and test data correlation," AIAA J. **1**, 1657–1659 (1963).

[5] Fielder, G., *Structure of the Moon's Surface* (Pergamon Press, Inc., New York, 1961).

[6] "Linde company superinsulation applied to space vehicles," Linde Co., Div. of Union Carbide, New York.

[7] "NRC-2 insulation," National Research Corp., Cambridge, Mass.

[8] Gaumer, R. and McKellar, L., "Thermal radiative control surfaces for spacecraft," Lockheed TR LMSD-704014 (March 1961).

[9] Pettit, E. and Nicholson, S. B., "Lunar radiation and temperatures," Astrophys. J. **71**, 102 (1930).

[10] Pettit, E., "Radiation measurements on the eclipsed moon," Astrophys. J. **91**, 408 (1940).

[11] Hamilton, D. C. and Morgan, W. R., "Radiation interchange configuration factors," NACA TN 2836 (1952).

[12] Kropschot, R. H. and Burgess, R. W., "Perlite for cryogenic insulation," *Proceedings of the 1962 Cryogenic Engineering Conference* (Plenum Press, Inc., New York, 1963), pp. 425–436.

[13] Wylie, C. R., *Advanced Engineering Mathematics* (McGraw-Hill Book Co., Inc., New York, 1951), p. 591.

[14] Scott, R. B., *Cryogenic Engineering* (D. Van Nostrand, Inc., Co., New York, 1959), p. 149.

[15] Lindquist, C. R. (Linde Co.) and Gray, W. A. (Martin Co.), personal communications (February 1962).

[16] Dempster, W. E., Evans, R. L., and Olivier, J. R., "Lunar storage of liquid propellant," NASA TN D-1117 (July 1962).

[17] Ruder, J. M., "Stratification in a pressurized container with sidewall heating," AIAA J. **2**, 135–137 (1964).